Proximity effects in conical-ferromagnet/superconductor bilayers

Chien-Te Wu,[1,*] Oriol T. Valls,[1,†] and Klaus Halterman[2,‡]

[1]*School of Physics and Astronomy, University of Minnesota, Minneapolis, Minnesota 55455, USA*

[2]*Michelson Lab, Physics Division, Naval Air Warfare Center, China Lake, California 93555, USA*

(Received 5 October 2012; revised manuscript received 2 November 2012; published 30 November 2012)

We present a study of various aspects of proximity effects in F/S (ferromagnet/superconductor) bilayers, where F has a spiral magnetic texture such as that found in holmium, erbium, and other materials, and S is a conventional s-wave superconductor. We numerically solve the Bogoliubov–de Gennes (BdG) equations self-consistently and use the solutions to compute physical quantities relevant to the proximity effects in these bilayers. We obtain the relation between the superconducting transition temperature T_c and the thicknesses d_F of the magnetic layer by solving the linearized BdG equations. We find that the $T_c(d_F)$ curves include multiple oscillations. Moreover, the system may be reentrant not only with d_F, as is the case when the magnet is uniform, but also with temperature T: the superconductivity disappears in certain ranges of d_F or T. The T reentrance reported here occurs when d_F is larger than the spatial period of the conical exchange field. We compute the condensation free energies and entropies from the full BdG equations and find the results are in agreement with T_c values obtained by linearization. The inhomogeneous nature of the magnet makes it possible for all odd triplet pairing components to be induced. We have investigated their properties and found that, as compared to the singlet amplitude, both the $m = 0$ and ± 1 triplet components exhibit long-range penetration. For nanoscale bilayers, the proximity lengths for both layers are also obtained. These lengths oscillate with d_F and they are found to be long range on both sides. These results are shown to be consistent with recent experiments. We also calculate the reverse proximity effect described by the three-dimensional local magnetization, and the local density of states, which reveals important energy-resolved signatures associated with the proximity effects.

DOI: 10.1103/PhysRevB.86.184517 PACS number(s): 74.45.+c, 74.62.−c, 74.25.Bt

I. INTRODUCTION

The emerging field of spintronics has stimulated interest in fabricating solid-state devices that make use of the intrinsic spins as a degree of freedom.[1] Strides have been made recently towards exploiting the spin variable in hybrid ferromagnet/superconductor (F/S) systems. Such systems have shown promise for a number of practical applications, including nonvolatile information storage. The simplest of such potential devices usually involve layered F/S heterostructures. Owing to these potentially important spintronic applications, research on the fundamental physics of these systems has received great attention in the last decade.[2,3] The most important basic physics elucidated by these studies is probably that of the superconducting proximity effects in F/S nanostructures,[3] which describe the interplay between ferromagnetic and superconducting order parameters. Although these two order parameters are rarely found to coexist naturally in bulk materials, such coexistence can be and has been achieved near the interfaces of artificially created F/S composites. Thus, the subject has become important not only for its technological applications, but also because of the underlying fundamental physics.

In elementary treatments, ferromagnetism is often deemed strictly incompatible with s-wave superconductivity due to their mutually exclusive order parameters. In ferromagnets, the exchange field tends to cause the electronic spins to align in the same direction, while in singlet s-wave superconductors, the Cooper pairs are composed of both spin-up and -down electrons. These two order parameters seem to naturally oppose each other. In fact, in F/S heterostructures this competition leads to a strong modification of the behavior of the superconducting Cooper-pair amplitudes. When a Cooper pair in S encounters an F/S interface and enters the F region, the momenta of spin-up and -down electrons that make up the Cooper pair are changed because of the exchange field in the F region. This leads to a nonzero center-of-mass momentum of the Cooper pair[4,5] and an overall damped oscillating Cooper-pair amplitude in the F side. It is because of these two competing order parameters that the oscillations decay over a relatively short length scale which decreases as the exchange field increases.

These oscillations of the superconducting wave functions are one of the most salient features governing proximity effects in F/S systems and form the basis for switching applications that require the manipulation of the superconducting transition temperature T_c through variation of the experimental parameters. Due to the oscillatory nature of the Cooper-pair amplitudes, the dependence of T_c on the thickness of the ferromagnetic layer d_F in F/S bilayers is oscillatory too. Furthermore, the interference between the transmitted pairing wave function through the F/S interface and the reflected one from the boundary can become fully destructive: the superconductivity disappears for a certain d_F range. This superconducting reentrant behavior with d_F has been found experimentally in Nb/$Cu_{1-x}Ni_x$ and Fe/V/Fe trilayers[6–8] and it is well understood theoretically.[3,9–14]

Another important fact about F/S proximity effects is the generation of induced triplet pairing correlations. These can be generated by the presence of spin active interfaces,[15–17] or (and this is the case we will focus on here) in systems with clean interfaces and inhomogeneous F structure.[18–22] The simplest such cases are $F_1/S/F_2$ or $F_1/F_2/S$ layers in which the magnetizations of the two F layers are misaligned. For s-wave superconductors, where the orbital part of the pair

wave function is even, the Pauli principle requires the spin part to be odd and this would appear to forbid the existence of triplet correlations. However, triplet correlations that are odd[23] in frequency (or equivalently in time[21]) can be induced in F/S systems, with S being s-wave pairing, without violating the Pauli exclusion principle.

The importance of odd triplet correlations lies in their long-range nature in the magnet, i.e., their proximity lengths can be in principle comparable to those found in the usual superconducting proximity effects involving nonmagnetic metals. Since the exchange fields tend to align the electronic spins of the Cooper-pair electrons, the proximity length for singlet pairing is very short (and dependent on the magnitude of exchange field). However, the triplet pairing correlations can involve electron pairs with both spins aligned along the local magnetization direction, and thus be much less sensitive to the mechanism of exchange fields, penetrating much deeper in F than their singlet counterparts. The possible appearance of both $m = 0$ and ± 1 (m denoting the usual spin quantum number) components of induced triplet correlations is controlled by the symmetry of the system and by conservation laws.[22] In multilayer F/S systems, when the F layers are magnetically homogeneous (all exchange fields are along the same direction, the quantization axis), only the total spin projection corresponding to the $m = 0$ component can be induced. On the contrary, all three components ($m = 0$ and ± 1) can arise if the direction of exchange fields differs in the ferromagnets, e.g., the exchange fields of F_1 and F_2 are not aligned in[22] $F_1/S/F_2$ or $F_1/F_2/S$ types of trilayers.[24] These long-range characteristics of triplet correlations have been experimentally detected in ferromagnetic multilayers by taking advantage of their magnetic inhomogeneity.[25–27]

Aside from ferromagnet misalignment, another possibility to generate long-range triplet correlations is to use a ferromagnet with an intrinsic inhomogeneous magnetic texture.[28] Such structures are inherent to either known elements or chemical compounds. Examples of this kind of ferromagnets include most prominently Ho,[29] which has a spiral magnetic structure at low temperatures. A similar spiral magnetic structure is found in metallic erbium,[30] MnSi thin films,[31] and Fe(Se,Te) compounds.[32] Indeed, it has been experimentally confirmed that long-range triplet correlations are induced in Nb/Ho/Co multilayers[33] with the periodicity of Ho playing an important role in triplet supercurrents. Superconducting phase-periodic conductance oscillations have also been observed in Al/Ho bilayers[29] where the thickness of Ho is much larger than the penetration length of singlet amplitudes. This finding can be explained in the framework of the triplet proximity effects. Theoretically, the spin-polarized Josephson current in S/Ho/S junctions has been studied[34] via quasiclassical Green's function techniques. The triplet supercurrent in Ho/Co/Ho trilayers was also investigated in the diffusive[35] and clean[36] regimes. The long-range effects can, however, be limited by interface quality and impurities.[37] These earlier works show that ferromagnets with an intrinsic spiral magnetic structure are of particular interest when studying superconducting proximity effects in F/S nanostructures. Generation of all triplet components in F/S systems where the F magnetic structure is inhomogeneous requires only a *single* F layer, an obvious advantage from the fabrication point of view. These components can also be induced in misaligned F/S structures with multiple uniform F layers, but the situation is different. Thus, in Ref. 24 we studied the switching effects and associated physics that occur in $F_1/F_2/S$ trilayers when the angle between exchange fields is varied. Here, motivated by the recent experiments mentioned above, we explore the importance of the geometry and the inherent spiral magnetism in a single-F-layer system.

It was also recently predicted[38] that superconductivity in conical-ferromagnet/superconductor bilayers can be reentrant *with temperature*, in addition to the standard reentrance with d_F mentioned above. It was shown via numerical solution of the Bogoliubov–de Gennes (BdG) equations that in certain cases superconductivity can exist in a range $T_{c1} < T < T_{c2}$, where T_{c1} is nonzero. This reentrance with temperature is quite different from that found in ternary rare-earth compounds such as $ErRh_4B_4$ and $HoMo_6S_8$,[39–43] where the disappearance of superconductivity below T_{c1} results from the onset of long-range ferromagnetism. In the bilayers considered in Ref. 38, the high-T phase and the low-T phase are the same. The physical reasons that account for the reentrance there are attributed to the proximity effects associated with the interference of Cooper-pair amplitudes and the generation of triplet pairing correlations, resulting in nontrivial competition between the entropies and condensation energies. This explains why we do not find[24] this reentrance in $F_1/F_2/S$ trilayers where the additional oscillatory mechanism associated with spiral ferromagnets is absent.

In this paper, we present results for various properties of the proximity effects in F/S bilayers, where the F layer has a helical magnetic structure. We numerically find the self-consistent solutions to the BdG equations[44] and use them to compute important physical quantities. By linearizing the BdG equations, we calculate the critical temperature as a function of magnet thickness, exchange-field strength and periodicity, and other parameters. We then discuss the effects of varying the superconductor thickness to coherence length ratio. We show that depending on the width of the superconductor, and for a broad range of magnetic strengths, reentrant behavior as a function of magnet thickness can arise. We find that under certain conditions, the superconductivity can also be reentrant with temperature, and for larger d_F values than previously reported.[38] To clarify these reentrant phenomena, we investigate the thermodynamic functions associated with the various ways reentrance can arise. We find that all components of the odd triplet correlations can be induced and we discuss their long-range nature. We then characterize the important triplet long-range behavior by introducing the corresponding proximity lengths. We find that these lengths oscillate as a function of d_F, and depend on details of the magnetic texture. Reverse proximity effects are also studied to determine the magnetic influence on the superconductor: we calculate the local magnetization vector revealing greater penetration into S for weaker exchange fields. Lastly, the spectroscopic information is presented by means of the local density of states to demonstrate consistency with the T_c results.

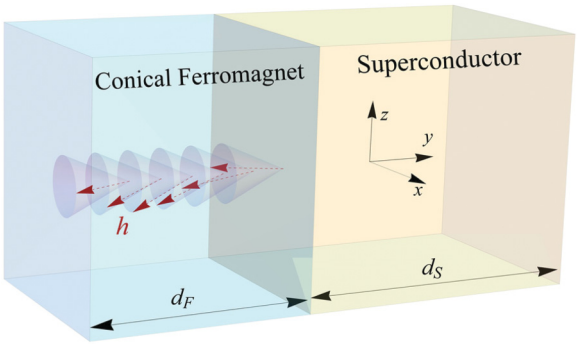

FIG. 1. (Color online) Diagram of the conical-ferromagnet/superconductor bilayer studied. The spiral magnetic structure is described by an exchange field $\boldsymbol{h}$ [see Eq. (1)]. The system is infinite in the x-z plane and finite in y. The relevant widths are labeled.

II. METHODS

The procedures we employ to self-consistently solve the BdG equations and to extract the relevant quantities are very similar to those already described in the literature (see Refs. 17 and 38 and references therein). It is unnecessary to repeat details here. We consider F/S bilayers that consist of one ferromagnetic layer with spiral exchange fields and a superconducting layer with s-wave pairing. The geometry is depicted in Fig. 1. Our systems are infinite in the x-z plane and finite along the y axis. Their total thickness is denoted by d: the F layer has width d_F and the S layer has width $d_S = d - d_F$. The left end of the bilayers is the $y = 0$ plane. We assume that the interface lies in the x-z plane and the exchange field $\mathbf{h}$, which is present only in F, has a component that rotates in this plane plus a constant component in the y direction, perpendicular to the interface:

$$\mathbf{h} = h_0 \left\{ \cos\alpha \hat{\mathbf{y}} + \sin\alpha \left[\sin\left(\frac{\beta y}{a}\right) \hat{\mathbf{x}} + \cos\left(\frac{\beta y}{a}\right) \hat{\mathbf{z}} \right] \right\}, \tag{1}$$

where the helical magnetic structure has a turning angle β and opening angle α. We will take a, the lattice constant, as our unit of length and vary the strength h_0. The spatial period of the helix is $\lambda = 2\pi a/\beta$.

The effective Hamiltonian of our system is

$$\begin{aligned} \mathcal{H}_{\text{eff}} = \int d^3r \Bigg\{ & \sum_{\rho} \psi_{\rho}^{\dagger}(\mathbf{r}) \left(-\frac{\nabla^2}{2m^*} - E_F \right) \psi_{\rho}(\mathbf{r}) \\ & + \frac{1}{2} \left[\sum_{\rho,\rho'} (i\sigma_y)_{\rho\rho'} \Delta(\mathbf{r}) \psi_{\rho}^{\dagger}(\mathbf{r}) \psi_{\rho'}^{\dagger}(\mathbf{r}) + \text{H.c.} \right] \\ & - \sum_{\rho,\rho'} \psi_{\rho}^{\dagger}(\mathbf{r}) (\mathbf{h}\cdot\boldsymbol{\sigma}) \psi_{\rho'}(\mathbf{r}) \Bigg\}, \end{aligned} \tag{2}$$

where ρ and ρ' are spin indices, $\psi_{\rho}(\mathbf{r})$ is the field operator, and $\boldsymbol{\sigma}$ are the Pauli matrices. $\Delta(\mathbf{r})$ in the above equation is the pair potential. To apply the BdG formalism to spatially inhomogeneous systems, we first invoke the generalized Bogoliubov[45] transformation $\psi_{\rho}(\mathbf{r}) = \sum_n [u_{n\rho}(\mathbf{r})\gamma_n + v_{n\rho}^*(\mathbf{r})\gamma_n^{\dagger}]$, where $u_{n\rho}(\mathbf{r})$ and $v_{n\rho}(\mathbf{r})$ are quasiparticle and quasihole wave functions and the creation operator $\gamma_n^{\dagger}$ and annihilation operator γ_n obey the usual fermionic anticommutation relations. By recasting the effective Hamiltonian into a diagonalized form, via the commutation relations between $\mathcal{H}_{\text{eff}}$ and field operators, and making use of the quasi-one-dimensional nature of the problem, one arrives at the BdG equations

$$\begin{aligned} & \begin{pmatrix} \mathcal{H}_0 - h_z & -h_x + ih_y & 0 & \Delta(y) \\ -h_x - ih_y & \mathcal{H}_0 + h_z & -\Delta(y) & 0 \\ 0 & -\Delta(y)^* & -(\mathcal{H}_0 + h_z) & h_x + ih_y \\ \Delta(y)^* & 0 & h_x - ih_y & -(\mathcal{H}_0 - h_z) \end{pmatrix} \\ & \times \begin{pmatrix} u_{n\uparrow}(y) \\ u_{n\downarrow}(y) \\ v_{n\uparrow}(y) \\ v_{n\downarrow}(y) \end{pmatrix} = \epsilon_n \begin{pmatrix} u_{n\uparrow}(y) \\ u_{n\downarrow}(y) \\ v_{n\uparrow}(y) \\ v_{n\downarrow}(y) \end{pmatrix}, \end{aligned} \tag{3}$$

where $\mathcal{H}_0 \equiv -\frac{1}{2m^*}\frac{\partial^2}{\partial y^2} + \epsilon_{\perp} - E_F$ is the usual single-particle Hamiltonian for the quasi-one-dimensional problem, with $\epsilon_{\perp}$ denoting the kinetic energy associated with the transverse direction. The self-consistency relation can be rewritten as

$$\Delta(y) = \frac{g(y)}{2} {\sum_n}' [u_{n\uparrow}(y) v_{n\downarrow}^*(y) - u_{n\downarrow}(y) v_{n\uparrow}^*(y)] \tanh\left(\frac{\epsilon_n}{2T}\right), \tag{4}$$

where $g(y)$ is the usual BCS superconducting coupling constant in the S region, and zero in the F material. The prime sign indicates summing over all eigenstates with eigenenergies less than or equal to a cutoff "Debye" frequency ω_D. The solutions to the BdG equations must be determined self-consistently. This self-consistency condition is extremely important in studying proximity effects.

The singlet pair amplitude, i.e., the amplitude for finding a Cooper pair $F(y)$, is given by $F(y) \equiv \Delta(y)/g(y)$. One can determine the superconducting transition temperatures T_c by looking for the temperatures at which the pair amplitudes becomes vanishingly small. However, it is much more efficient to find T_c by linearizing the self-consistency relation (4) and using a perturbation expansion. This technique has been discussed in other papers[38,46] and the details are not repeated here.

Once a full set of self-consistent solutions is obtained, all the additional quantities of interest can be computed. For example, the triplet correlations corresponding to $m = 0$ and $m = \pm 1$, respectively,[21,22] can be written, with our geometry and phase conventions, in terms of the quasiparticle and quasihole wave functions as

$$f_0(y,t) = \frac{1}{2} \sum_n [u_{n\uparrow}(y) v_{n\downarrow}^*(y) + u_{n\downarrow}(y) v_{n\uparrow}^*(y)] \zeta_n(t), \tag{5a}$$

$$f_1(y,t) = \frac{1}{2} \sum_n [u_{n\uparrow}(y) v_{n\uparrow}^*(y) - u_{n\downarrow}(y) v_{n\downarrow}^*(y)] \zeta_n(t), \tag{5b}$$

where $\zeta_n(t) \equiv \cos(\epsilon_n t) - i \sin(\epsilon_n t) \tanh[\epsilon_n/(2T)]$. As discussed in Sec. I, both f_0 and f_1 have to vanish at $t = 0$ to comply with the Pauli principle. However, in general both of

them can be induced when $t \neq 0$ and the magnetic structure is inhomogeneous.

One is also able to evaluate the thermodynamic quantities from the free energy $F(T)$. For an inhomogeneous system, it is computationally most convenient to use the expression[47]

$$F(T) = -2T \sum_n \ln\left[2\cosh\left(\frac{\epsilon_n}{2T}\right)\right] + \left\langle \frac{\Delta^2(y)}{g(y)} \right\rangle_s, \quad (6)$$

where $\langle \ldots \rangle_s$ denotes spatial average. The condensation free energy ΔF is the difference between the free energies of the superconducting state F_S and the normal states F_N, $\Delta F = F_S - F_N$.

Another important physical quantity, which can be determined experimentally by tunneling spectroscopy, is the local density of states (LDOS). This quantity often reveals important information about the superconducting features of the sample studied. In our quasi-one-dimensional model, the LDOS $N(y,\epsilon)$ depends spatially only on y. It can be easily rewritten, as shown, e.g., in Refs. 5 and 46, in terms of the wave functions.

Just as the superconducting order parameter is changed by the presence of ferromagnets, also, near the interface, the ferromagnetism can be modified by the presence of the superconductor,[5,48–53] a phenomenon known as the reverse proximity effect. It is best described by considering the local magnetization **m**, which is in our case three dimensional. In terms of the wave functions, its components can be written as

$$m_x(y) = -\mu_B \sum_n \{[u^*_{n\uparrow}(y)u_{n\downarrow}(y) + u^*_{n\downarrow}(y)u_{n\uparrow}(y)]f_n + [v_{n\uparrow}(y)v^*_{n\downarrow}(y) + v_{n\downarrow}(y)v^*_{n\uparrow}(y)](1-f_n)\}, \quad (7a)$$

$$m_y(y) = i\mu_B \sum_n \{[u^*_{n\uparrow}(y)u_{n\downarrow}(y) - u^*_{n\downarrow}(y)u_{n\uparrow}(y)]f_n + [v_{n\uparrow}(y)v^*_{n\downarrow}(y) - v_{n\downarrow}(y)v^*_{n\uparrow}(y)](1-f_n)\}, \quad (7b)$$

$$m_z(y) = -\mu_B \sum_n \{[|u_{n\uparrow}(y)|^2 - |u_{n\downarrow}(y)|^2]f_n + [|v_{n\uparrow}(y)|^2 - |v_{n\downarrow}(y)|^2](1-f_n)\}, \quad (7c)$$

where f_n is the Fermi function of ϵ_n and μ_B is the Bohr magneton.

III. RESULTS

In the results shown here, capital letters will always denote the dimensionless lengths denoted by the corresponding small letter. For example, the dimensionless thickness of the ferromagnet is written as $D_F \equiv d_F/a$ and that of superconductors is $D_S \equiv d_S/a$, where a is the lattice constant in Eq. (1). For the helical magnetic structure, we take angular values [see Eq. (1)] $\alpha = 4\pi/9$ and $\beta = \pi/6$ which are[29,54] appropriate to Ho, in which case $D_F = 12$ contains one full period of the spiral exchange field. We will denote this dimensionless spatial period by Λ in the following sections. For materials other than Ho, many of the results can be read off by rescaling Λ to the appropriate value. Throughout this paper, the dimensionless superconducting coherence length is fixed to be $\Xi_0 = 100$. In the same spirit, the dimensionless exchange field I is measured in terms of the Fermi energy: $I \equiv h_0/E_F$. We choose the Fermi wave vector in S to equal $1/a$. We take the "Debye" cutoff value to be $\omega_D = 0.04E_F$. As usual, this value is irrelevant except for setting the overall transition temperature. Temperatures are given in dimensionless form in terms of T_c^0, the transition temperature of bulk S material. When discussing the triplet amplitudes, which are time dependent, we use the dimensionless time $\tau \equiv t\omega_D$. Vertical dashed lines shown in figures, when present, denote the F/S interface.

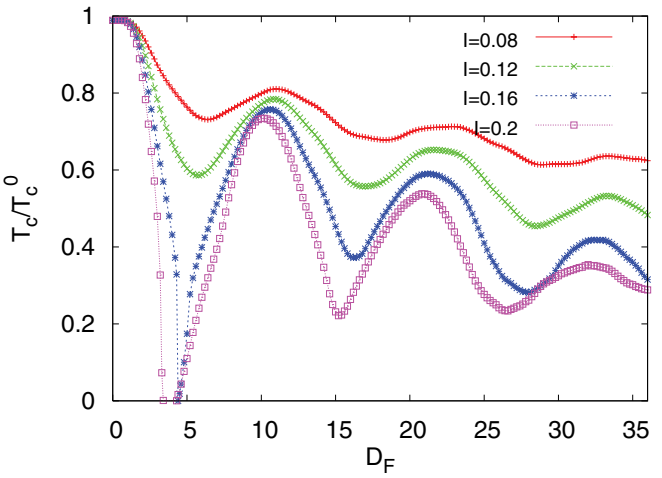

FIG. 2. (Color online) Calculated transition temperatures T_c, normalized to T_c^0, vs D_F for several values of the dimensionless exchange field I (see text). In this figure, D_S is fixed for all values of I to be $1.5\Xi_0$. The lines connecting data points are guides to the eye.

A. Transition temperatures

To investigate the details of the predicted oscillatory nature of the d_F dependence of T_c as discussed in Sec. I, we calculated T_c as a function of D_F for several I and D_S values. These results are shown in Figs. 2 and 3. The D_F

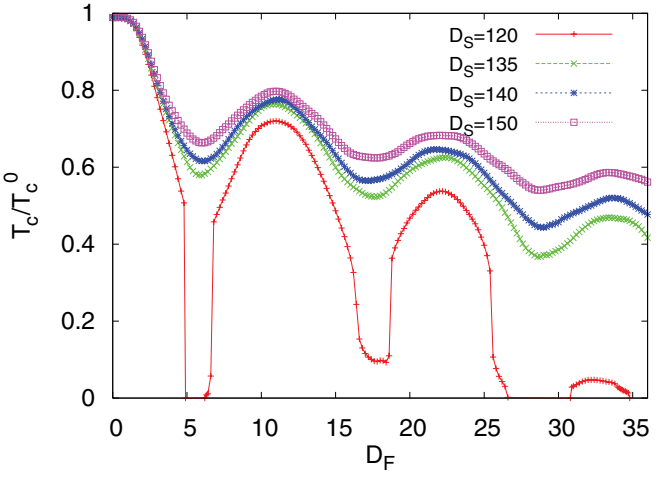

FIG. 3. (Color online) Transition temperatures T_c vs D_F at $I = 0.1$ and several D_S. The lines are guides to the eye.

range in both figures includes three complete periods of the spiral magnetic order. This is reflected in the results shown: indeed, the presence of multiple oscillations in the included range of D_F is the most prominent feature in Figs. 2 and 3. The oscillations in T_c arise (as we discuss below) from a combination of the periodicity of the spiral magnetic structure and the usual T_c oscillations which arise, even when the magnet is uniform, from the difference[3,4] in the wave vectors of the up and down spins. In Fig. 2, one can also see that with stronger exchange fields, the oscillation amplitudes are larger. Despite this increase of the amplitudes with the exchange field (they are approximately proportional to I), the overall T_c decreases when the exchange field increases. This is consistent with expectations: a stronger exchange field destroys the superconductivity more efficiently. As mentioned in Sec. I, when the exchange field is strong enough, the systems can become normal in some range $D_{F1} < D_F < D_{F2}$. Indeed, reentrance with d_F can be seen to occur in Fig. 2 near $D_F = 4$ at $I = 0.2$. Another feature seen in this figure is the decrease of the amplitude oscillations with increasing D_F. This arises simply because the singlet Cooper-pair amplitudes in S near the F/S boundary decay more strongly at larger d_F and therefore the effect of the pair-amplitude oscillations in F is weaker.[55]

In a F/S bilayer where the ferromagnet is homogeneous, the periodicity of the T_c oscillations is governed by the exchange field, or equivalently, by the magnetic coherence length[5] $\Xi_F = 1/I$. Here, where a bilayer with a conical inhomogeneous ferromagnet is considered, the intrinsic spiral magnetic order with spatial period Λ plays an equally important and competing role in the T_c oscillations. In other words, both the strength and the periodicity of exchange fields influence the overall decay and the oscillatory nature of the superconducting transition temperatures. The existence of two different spatial periodicities leads to the obvious consequence that the $T_c(D_F)$ curves are not describable in terms of one single period. However, when I is not very strong ($I \lesssim 0.1$), the minima of T_c are near the locations where $D_F = \Lambda/2$, $3\Lambda/2$, and $5\Lambda/2$ and similarly, the T_c maxima occur near $D_F = \Lambda$, 2Λ, and 3Λ. This indicates that the magnetic periodicity is dominant. Roughly speaking, the maxima and the minima are correlated with the strongest and weakest spatial average of the exchange field components in F. As I increases and Ξ_F decreases, deviations become obvious. Figure 2 shows that the distances between two successive maxima decrease when the exchange fields increase.

The existence of the multiple oscillations discussed above has been confirmed experimentally. In Ref. 56, T_c in Nb/Ho bilayers was measured as a function of d_F. The results exhibit an overall decay with Ho thickness, on which there are superimposed oscillations which are correlated with, but not simply described by, the spatial wavelength λ of the Ho structure. Comparison with the theory discussed here was made, using I as an adjustable parameter. Values near $I = 0.1$ were found to provide the best fit. The other parameters were extracted from other known properties of Ho and Nb or (e.g., d_S) from the experimental sample geometry. The results of the comparison were extremely satisfactory, showing clear agreement in all the features of the rather intricate $T_c(d_F)$ experimental curves. It was found also that one of the samples was close to being reentrant with d_F at a value very close to that predicted by theory.

In Fig. 3, we present T_c results for several values of D_S ranging from $1.2\Xi_0$ to $1.5\Xi_0$, with a fixed exchange field $I = 0.1$. One can see that the distance between successive maxima is an extremely weak function of D_S. This agrees with our previous discussion: the oscillatory nature in T_c is chiefly dependent on the exchange fields and magnet structure. Since superconductivity is more robust for larger D_S, the ferromagnet lowers the overall T_c for thinner superconductors as evidenced in Fig. 3. Figure 3 also demonstrates that not only a strong I can lead to D_F reentrances, but also a thinner D_S. Interestingly, at the smallest value of D_S considered, there are two D_F reentrance regions, one near $D_F = 5$ and the other near $D_F = 27$. As discussed above, these D_F reentrances in both Figs. 1 and 2 are mainly due to the interference between the transmitted and reflected Cooper-pair condensates that are oscillatory in the F region.

In previous work,[38] we reported one specific case where superconductivity in Ho/S bilayers exhibits not only the usual reentrance with d_F but also, at some fixed values of d_S, h_0, and d_F, reentrance with T, that is, superconductivity exists only in a temperature range $T_{c1} < T < T_{c2}$, where T_{c1} is finite. In the example reported in Ref. 38, temperature reentrance occurred near the first minimum of the $T_c(D_F)$ curve. We have investigated here whether this kind of reentrance can occur near some of the other minima of $T_c(D_F)$. These locations appear favorable for such an occurrence since superconductivity is relatively weak near these minima. Also, reentrance with D_F is after all an extreme case of a minimum $T_c(D_F)$. We have found that other T-reentrant examples can indeed be found, although by no means universally. Here, we report another example of reentrance occurring near the second minimum of $T_c(D_F)$. At this larger value of D_F, it should be much easier to grow Ho in the spiral structure. In Fig. 4, the main plot shows $T_c(D_F)$ for the parameter values specified in the caption. The first minimum of $T_c(D_F)$ drops to zero and is an example of D_F reentrance. In the region near the second minimum (green symbols) reentrance with T occurs. The region of interest is enlarged in the inset. There, the upper (green) symbols represent T_{c2} and the small dome of lower (blue) circles represent T_{c1}. In the dome region, but not outside it, the superconductivity is reentrant in T. When one lowers the temperature from the normal region, the F/S bilayers become superconducting at T_{c2}. With further cooling, the bilayers return to normal state. Reentrance in this case occurs at the second minimum rather than the first because there is no upper transition associated with the first minimum: the system is normal. Near the second minimum, the oscillatory effects are not as strong, and as as a result, the system becomes reentrant in T. This can be viewed as a "compromise": near the second minimum, as opposed to the first, superconductivity is not completely destroyed but it becomes "fragile" and can disappear upon lowering T. The physics involved from the thermodynamic point of view will be discussed in the following section.

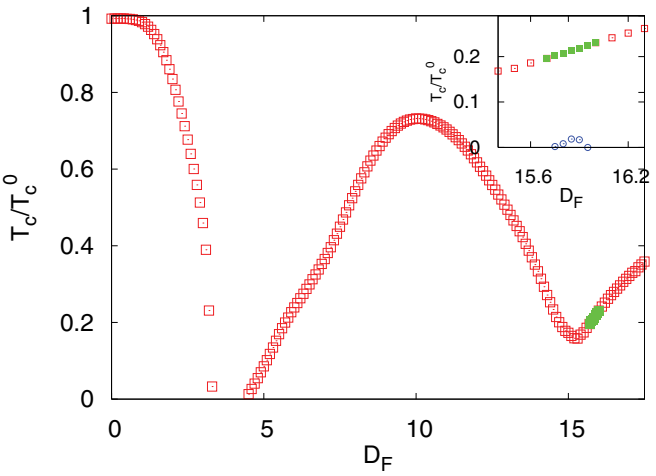

FIG. 4. (Color online) Calculated transition temperatures T_c vs D_F for $D_S = 148$ and $I = 0.2$. The main plot shows (red symbols) the overall T_c behavior from $D_F = 0$ to 1.5Λ. Reentrance with D_F near $D_F = 4$ is seen. In this case, there is also reentrance with temperature in the region indicated by (green) symbols near $D_F = 16$. The inset is a blowup of this region: superconductivity exists only in the region $T_{c1} < T < T_{c2}$, where T_{c2} is depicted by the upper (green) squares and T_{c1} by the (blue) circles.

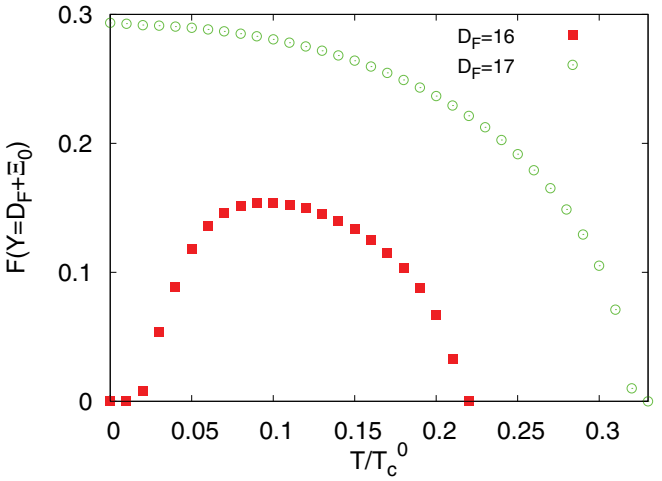

FIG. 5. (Color online) The singlet pair amplitude, normalized to its value for bulk S material, at a location one coherence length inside S from the Ho/S interface, plotted as a function of T. The (red) squares are for $D_F = 16$ and the (green) circles are for $D_F = 17$. All other parameters are as in Fig. 4.

B. Thermodynamics of reentrance phenomena

To understand the reentrance phenomena in T it is most useful to examine the thermodynamics of the two transitions, and in the region between them. From the condensation free energy ΔF, which can be evaluated as explained in connection with Eq. (6), other quantities such as the condensation energy and entropy are easily obtained. For reentrance with D_F, it is sufficient to look at the free energy at constant low T.

Considering the reentrance with T, it is illuminating to consider first the T dependence of the singlet pair amplitude $F(Y)$ well inside the S material. Thus, we focus on $F(Y)$ one coherence length from the interface: $Y = D_F + \Xi_0$. This quantity, normalized to its value in bulk S material, is plotted in Fig. 5 as a function of T for two contrasting values of D_F, one at $D_F = 16$ where reentrance occurs (see Fig. 4) and at a very nearby value $D_F = 17$, which lies just outside the reentrance region and exhibits typical behavior. Figure 5 (green circles) demonstrates that in the latter case the amplitude behaves qualitatively as the order parameter does in a conventional BCS superconductor: it decreases very slowly near $T = 0$ and eventually drops to zero very quickly but continuously near T_c, indicating the occurrence of a second-order phase transition. This transition occurs at $T_c/T_c^0 = 0.32$ in agreement with Fig. 4. However, the behavior of the pair amplitude in the reentrant region (red squares in Fig. 5) is quite different. There are two transition temperatures: below a very low but finite temperature $T_{c1}/T_c^0 = 0.02$, the singlet pair amplitude vanishes and the system is in its normal state. $F(Y)$ then begins to rise continuously, has a maximum at a temperature T_m (where $T_m/T_c^0 \approx 0.1$) and eventually drops to zero, again continuously, at an upper transition $T_{c2}/T_c^0 \approx 0.22$. In the region $T_{c1} < T < T_{c2}$, the system is in the superconducting state. Both transitions are of second order. The values of T_{c1} and T_{c2} from the vanishing of the amplitude, seen in Fig. 5, agree with those calculated directly from linearization of the self-consistent equation plotted in Fig. 4.

We now turn to the condensation free energy ΔF and entropy ΔS for the same T reentrant case. ΔF is shown in the top panel of Fig. 6 as calculated from Eq. (6) and normalized by $2E_0$, where E_0 is the condensation energy of bulk S material at $T = 0$. The lower panel shows the normalized condensation entropy, defined as the $\Delta S \equiv -d\Delta F/d(T/T_c^0)$. The meaning of the symbols in this figure is the same as in the previous one. When the system is near (but outside) the reentrant region, the behavior of both quantities plotted is qualitatively the same as that found in textbooks for bulk BCS superconductors. Quantitatively, the magnitude of ΔF for our systems is much smaller than that for bulk S where we would have $\Delta F = -0.5$ at $T = 0$ in our units. The value of T_c in the nonreentrant case can also be identified from where the free energies of the normal and superconducting states are the same [$\Delta F(T) \equiv 0$], and it agrees with both Figs. 4 and 5. Moreover, the vanishing of the entropy difference at a finite T_c confirms the occurrence of a second-order phase transition. The value of this transition temperature is consistent with all above results.

The story for the reentrant case is quite different. There, although the values of ΔF are much smaller compared to those in the standard case, one can still find that the minimum of ΔF occurs at approximately the same value T_m where the singlet pair amplitudes have a maximum. Thus, the superconductivity is most robust at $T = T_m$. The two transition temperatures T_{c1} and T_{c2} can also be determined from the top panel of Fig. 6 and match with those found in Figs. 4 and 5. In the two T ranges $T < T_{c1}$ and $T > T_{c2}$, the normal state is the only self-consistent solution to the basic equations, as is evident from Fig. 5. The vanishing ΔF when $T < T_{c1}$ means that the electrons do not then condensate into Cooper pairs. This is exactly what happens for pure superconductors when $T > T_c$.

There are some remarkable facts about the behavior of ΔS in the reentrant case. First, the vanishing of ΔS (along with

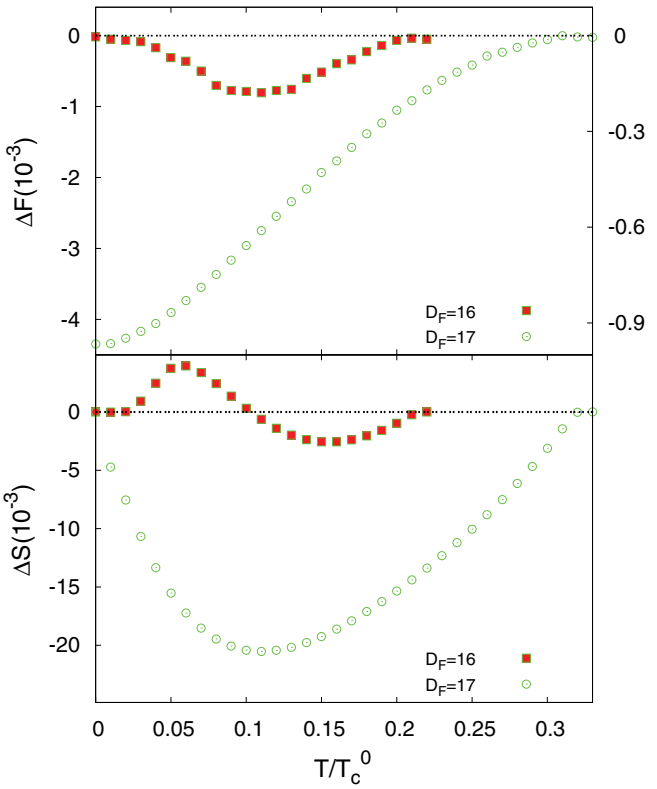

FIG. 6. (Color online) The normalized condensation free energies $\Delta F = F_S - F_N$ vs T/T_c^0 are shown in the top panel for the same cases presented in Fig. 5. The (red) squares and right scale are for $D_F = 16$. The (green) circles and left scale are for $D_F = 17$. The bottom panel shows the normalized (see text) entropy differences $\Delta S = S_S - S_N$ vs T/T_c^0 on the same vertical scale. The meaning of the symbols is the same as in the top panel.

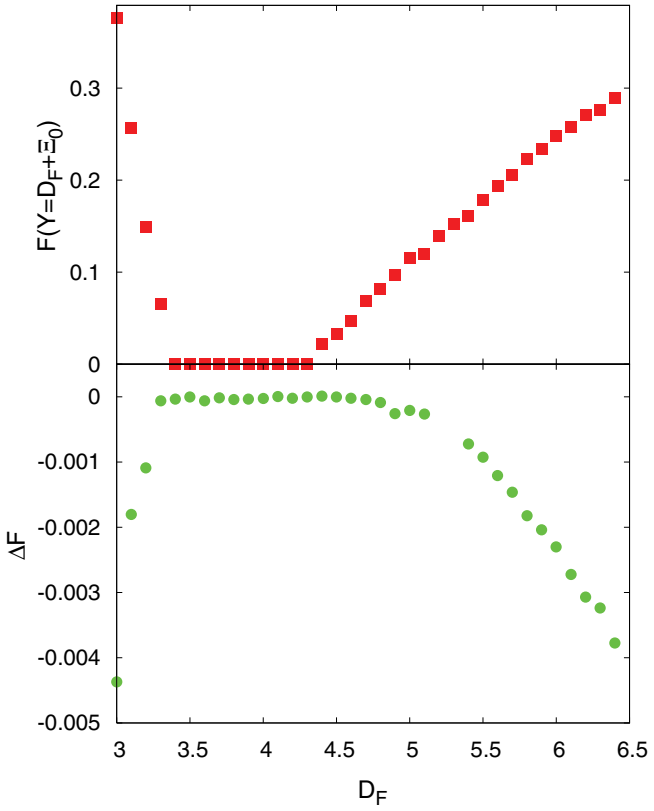

FIG. 7. (Color online) Reentrance with D_F. Top panel: normalized singlet pair amplitude, computed at a location one coherence length inside S from the interface, as a function of D_F. Bottom panel: normalized condensation free energy $\Delta F = F_S - F_N$ vs D_F at $T = 0$.

that of ΔF) in Fig. 6 indicates that the system undergoes second-order phase transitions at both T_{c1} and T_{c2}. Also, ΔS is positive for $T_{c1} < T < T_m$ where T_m is again the value of T at which the singlet pair amplitude reaches its maximum *and* ΔF its minimum. That the entropy of the superconducting state is higher than that of the normal state indicates that the normal state at $T_{c1} < T < T_m$ is *more* ordered than the superconducting one. This truly unusual fact, which is the root cause of the reentrance, is due to the oscillating nature of both the Cooper-pair condensates and of the exchange field, which leads to an uncommonly complicated structure for the pair amplitude. Above T_m, the superconducting state becomes more ordered than the normal state: ΔS is negative. From Figs. 5 and 6, we see that the singlet pair amplitudes, the condensation free energies, and entropy differences of reentrant case in the range $T_m < T < T_{c2}$ have a similar trend to those of the nonreentrant case in the range $0 < T < T_c$. We have found also examples of nonreentrant cases in which there is a finite temperature T_m at which ΔF has a minimum but where, on further lowering T, ΔF remains negative all the way to $T = 0$.

The situation in the more common D_F reentrance region, where we find that the system does not become superconducting when it is heated from $T = 0$, is different from that of T reentrance. A case where T_c vanishes in the range $D_{F1} < D_F < D_{F2}$ for $I = 0.2$ was seen in Fig. 2. To further analyze this D_F reentrance, we again calculated the singlet pair amplitudes inside S at one coherence length from the interface, in the zero-temperature limit. The top panel of Fig. 7 shows the normalized $F(D_F + \Xi_0)$ as a function of D_F, for the same parameters as the $I = 0.2$ case in Fig. 2. The singlet amplitudes drop to zero in the same range as where T_c vanishes in Fig. 2: the normal state is the only self-consistent solution and the superconductivity is completely destroyed in this D_F range. One can also see that the order parameter is continuous but its derivative discontinuous at D_{F1} and D_{F2}. In the bottom panel, we plot the corresponding condensation free energies (at $T = 0$) as a function of D_F. The D_F range and the temperature are the same as the top panel. The condensation free energies vanish in the same D_F reentrance region although their extreme smallness (at the level of our numerical uncertainty as can be gauged by the size of the points) at slightly larger values of D_F makes it difficult to verify in this panel that the regions are exactly the same. Unlike the derivatives of the singlet pair amplitudes, the derivatives of ΔF at D_{F1} and D_{F2} appear to be continuous.

The physical origins of these two kinds of reentrance are not identical. As mentioned in Sec. I, the interference effects of oscillating Cooper-pair wave functions are responsible for the D_F reentrance, provided that I is strong and D_F is not too thick. D_F reentrance does not require a nonuniform magnet. The conical-ferromagnet structure introduces an

additional nonuniform magnetic order which may coexist with nonuniform superconductivity as predicted in Ref. 57. This additional nonuniformity, with its concomitant introduction of triplet correlations and of a new periodicity, can produce, as we have shown, reentrant behavior in T, as opposed to the simpler behavior seen, e.g., near the first minimum in the main plot of Fig. 4. Thermodynamically, the reentrance with T is due to the competition between entropy and energy,[38] and driven by the high entropy of the disordered superconducting state. When $T < T_m$, ΔS is positive and the roles of the normal and superconducting phases are exchanged: the high-entropy phase is the superconducting one. Further lowering T brings the system back to normal state. One can compare the instance of T reentrance reported here with that reported in our previous work[38] where it occurs near the first minimum of $T_c(D_F)$. In that work, $D_S = 150 = 1.5\Xi_0$ and $I = 0.15$. Here, not only is D_S thinner but also I is greater. The first minimum of $T_c(D_F)$ in the main plot of Fig. 4 drops to zero and becomes a D_F reentrance region. Because stronger I and thinner D_S are unfavorable to superconductivity, the system can not sustain T reentrance there. Thus, a delicate balance of geometrical and material parameters is required.

C. Singlet to triplet conversion

In this section, we will discuss the general properties of the induced triplet pairing correlations in F/S bilayers with F being a conical ferromagnet. As mentioned in Sec. I, in the presence of inhomogeneous exchange fields in the F layers both the $m = 0$ and the $m = \pm 1$ triplet pair amplitudes are *allowed* by conservation laws and the Pauli principle, but this says *nothing* about their size or shape, or indeed on whether they will exist at all. Thus, detailed calculations are needed. The intrinsically inhomogeneous magnetic textures discussed here provide unique opportunities to study the triplet proximity effects in F/S systems containing only a single F layer. Triplet correlations in the ballistic regime for both $F_1/S/F_2$ and $F_1/F_2/S$ trilayers have been found in previous work[21,22,24] to be long ranged, and the expectation[33] that they will also be in our case is fulfilled. We will here discuss and characterize this and other aspects (such as the effect of the strength of the exchange fields on the triplet pair amplitudes) of triplet pairing correlations in F/S bilayers where the magnets maintain a spiral exchange field. Results presented in this section are all in the low-T limit.

To exhibit the long-range nature of both types of triplet amplitudes, we show in Fig. 8 both the triplet and singlet pair amplitudes for a thick F layer as a function of position, as given by the dimensionless coordinate Y. In this (and the next figure, Fig. 9), we will focus on the real parts of the in general complex [see Eqs. (5)] f_0 and f_1 since we have found that, for the cases shown, their imaginary parts are smaller by at least a factor of 2 to 5 and their behavior is similar to that of the real parts. To properly compare singlet and triplet quantities, both the singlet amplitude $F(Y)$ and the triplet amplitudes are normalized the same way: to the value of the singlet amplitude in bulk S material. For visibility, we have multiplied the triplet pair amplitudes by a factor of 10. In the

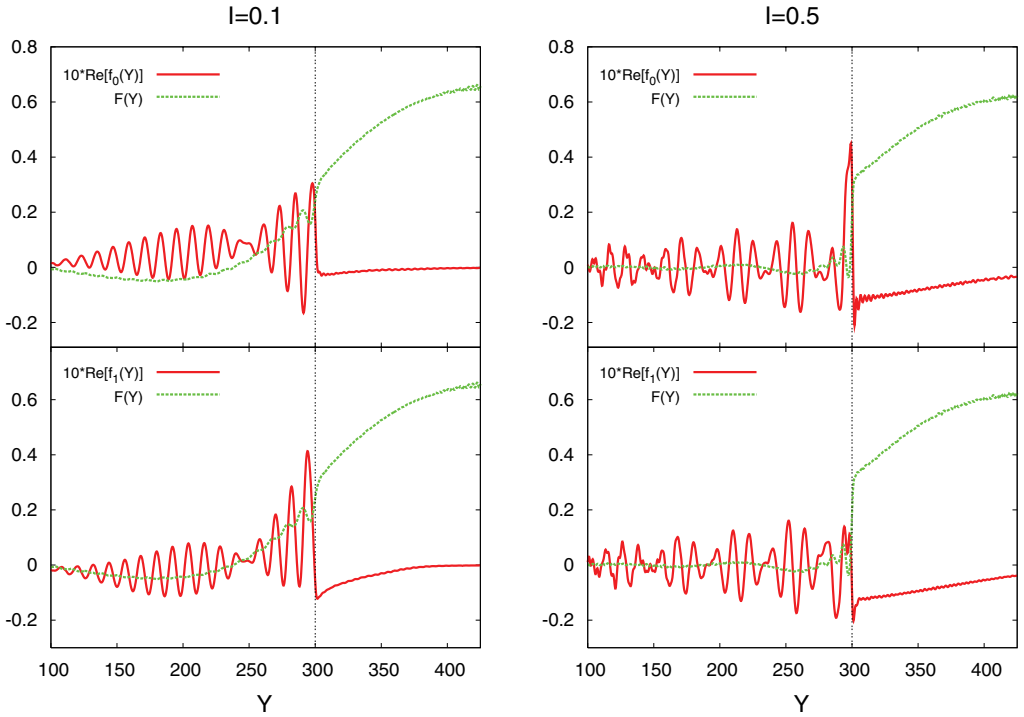

FIG. 8. (Color online) Comparison between the spatial dependencies of the singlet pair amplitude and the induced triplet correlations at the two indicated values of I, at $D_S = 150$, $D_F = 300$, and $T = 0$. The S region is to the right of the dashed vertical line. Both singlet $F(Y)$ (green curves higher in the S region) and triplet $f_0(Y)$, $f_1(Y)$ pair amplitudes are normalized to the value of $F(Y)$ in pure bulk S material. For this comparison, the normalized induced triplet pair amplitudes, which are evaluated at $\tau = 9.6$, are multiplied by a factor of 10. The real parts of $f_0(Y)$ and $f_1(Y)$ are shown (red curves strongly oscillating in the F region).

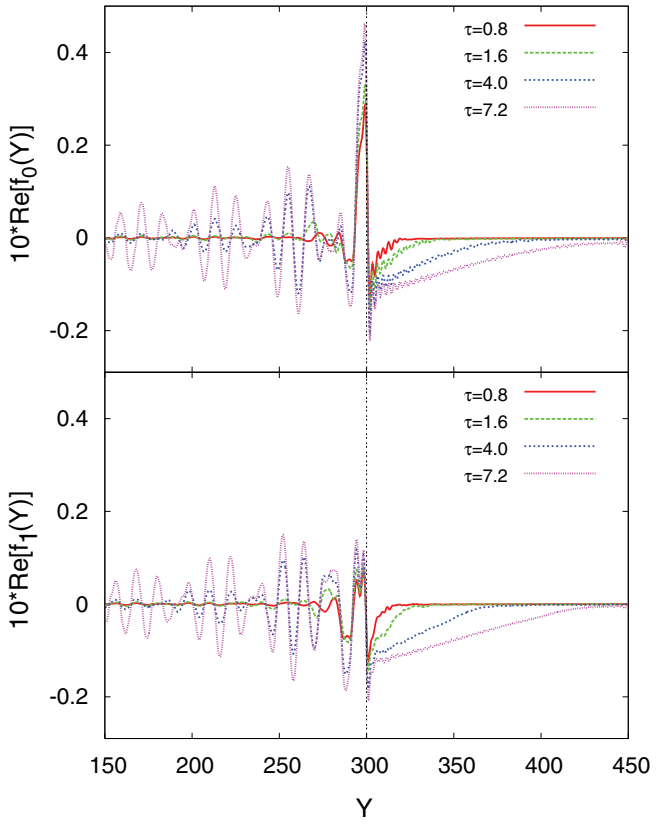

FIG. 9. (Color online) Real parts of the induced triplet pair amplitudes, normalized as in the previous figure, for different characteristic times τ. In these plots, $D_S = 150$, $D_F = 300$, and $I = 0.5$. The top panel shows the real part of $f_0(Y)$ and the bottom one that of $f_1(Y)$.

left and right columns of Fig. 8, we show in this way the real parts of both f_0 and f_1 when $I = 0.1$ and 0.5, respectively. The ferromagnet has a large thickness: $D_F = 3\Xi_0 = 2D_S$. The triplet correlations, which we recall vanish at equal times, are computed at a value of the dimensionless time $\tau = 9.6$. One sees right away that both the f_0 and f_1 components can be induced at the same time. This is always the case in our structures, as opposed to what occurs in $F_1/F_2/S$ and $F_1/S/F_2$ trilayers where the f_0 and f_1 components can be induced simultaneously only when the exchange fields in these F layers are noncollinear. Second, the induced triplet correlations on the F side are long ranged compared to the singlet amplitudes. The singlet amplitudes decay with a short[5] proximity length $2\pi\,\Xi_F \approx 2\pi/I$ due to the pair-breaking effect of the exchange field. In contrast, the proximity length for the triplet amplitudes as seen in Fig. 8 is much longer: it is of the order of Ξ_0, and does not depend strongly on I. The triplet amplitudes spread over the F side with an oscillatory behavior. This difference is more pronounced in the $I = 0.5$ case, where the decay length Ξ_F is much shorter than Ξ_0 and the singlet amplitudes diminish much faster than in the $I = 0.1$ case. For both $I = 0.1$ and 0.5, one can also see that the singlet amplitudes begin to rise from the F/S interface and saturate in the S side about one superconducting coherence length from the interface. This agrees with our previous work.[5] Another interesting feature seen in the $I = 0.5$ case is that the peak height of the f_1 component near the interface is not much higher than that of its other peaks, as happens with its f_0 counterpart. In other words, the subsequent peak heights in the F regions are comparable to those of the peak nearest to the interface.

In delineating the role of triplet correlations in other experimentally relevant quantities, it is necessary to understand their time dependence. Due to the self-consistent nature of the proximity effects and the fact that the triplet condensate amplitudes are odd in time, their time dependence is in general nontrivial. We illustrate this in Fig. 9, where we show the spatial dependence of both the $m = 0$ and ± 1 components of the triplet amplitude for several τ. The parameters used here are the same as in the right panels ($I = 0.5$) of Fig. 8. For easier comparison with Fig. 8, we have again multiplied the normalized triplet amplitudes by a factor of 10. Figure 9 shows that at small times triplet correlations are generated only near the interface. (We have of course verified that they always vanish when $\tau = 0$.) One can extract information about the proximity length from the growing increase of peak heights in the F regions. The peak heights grow faster when they are deeper inside the ferromagnet. Moreover, Fig. 9 clearly demonstrates that the triplet correlations penetrate into F regions as τ increases, in the range studied. More remarkably, the peaks of the f_1 component that are not nearest to the interface grow very fast in time and have heights that are comparable to the one nearest to the interface, consistent with our remarks in our discussion of Fig. 8. In contradistinction with the oscillating behavior of the triplet amplitudes in the F regions, one can see that both f_0 and f_1 decay monotonically into the S side without any oscillations. However, the triplet correlations still spread over in the S regions at larger values of τ just as they do in the F layer.

In the above paragraphs, we have discussed the long-range nature and other properties of the triplet amplitudes in our system when the conical ferromagnet is very thick. In the following paragraphs, we will consider the proximity effect of induced triplet pairing correlations for smaller-scale conical ferromagnets. To quantify the effect, we introduce a set of proximity lengths $L_{i,M}$ defined as

$$L_{i,M} = \frac{\int_M dY\,|f_i(Y,\tau)|}{\max_M |f_i(Y,\tau)|}, \quad i = 0,1, \quad M = S,F. \tag{8}$$

Here, the first index denotes the spin component, and the second index M denotes the region in which the given function is evaluated. If the decays were exponential, these lengths would coincide with the characteristic length in the exponent. Obviously, in the present situation, the decays are more complicated but the $L_{i,M}$ can easily be extracted numerically. They depend on D_S, D_F, I, and τ. The range of D_F we will consider is from Λ to 3Λ. In Fig. 10, we plot these proximity lengths on both the F and S sides for three different values of I, at $\tau = 4.0$. The left panels show the f_0 proximity lengths and the right panels that extracted from f_1. Recall that $I = 1$ corresponds to the half-metallic limit. We consider first the F side (top two panels). One can clearly see that both $L_{0,F}$ and $L_{1,F}$ are correlated to the strength of the exchange fields. Figure 10 displays a period of near $\Lambda/2$ for both $L_{0,F}$ and $L_{1,F}$ at $I = 1.0$. We also see that the peak heights increase

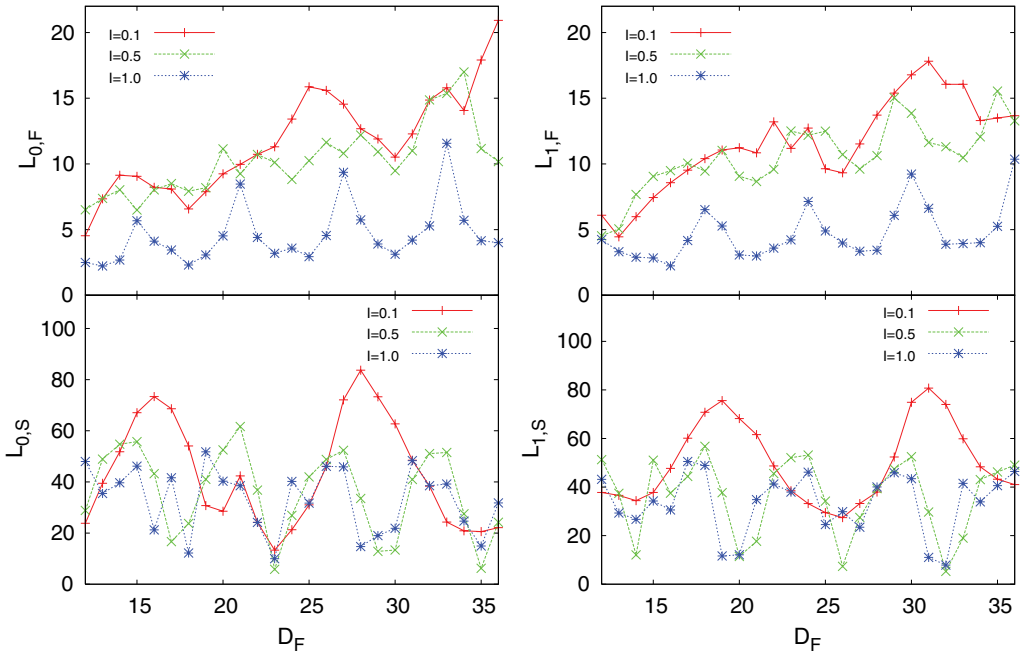

FIG. 10. (Color online) The proximity lengths $L_{i,M}$ [see Eq. (8)] of the induced triplet pair amplitudes vs D_F for different I, at $\tau = 4.0$ and $D_S = 150$. The left panels show the proximity lengths $L_{0,F}$ and $L_{0,S}$ (from f_0 in the F and S regions) and the right panels $L_{1,F}$ and $L_{1,S}$, similarly extracted from f_1. The lines are guides to the eye.

only slowly with increasing D_F. Also, the locations of the maxima or minima of $L_{0,F}$ are locations of minima or maxima, respectively, of $L_{1,F}$. This is as one might expect from the rotating character of the field. On the other hand, for $I = 0.1$ or 0.5, the periodicity is not clear since, for reasons already mentioned, the intermingling of periodicities becomes more complicated. Overall, the proximity lengths are larger than those in the half-metallic limit. However, one can still say that both $L_{0,F}$ and $L_{1,F}$ gradually increase, although with fluctuations, with D_F.

The superconductor on the S side is intrinsically s wave but because of the F layer, triplet correlations can be induced in it, near the interface, as seen in Figs. 8 and 9. Their decay, which is now monotonic, can be equally characterized by the proximity lengths defined in Eq. (8). Results are plotted in the bottom panels of Fig. 10. The minimum of $L_{0,S}$ is, for all three values of I, at $D_F = 23$ which is near 2Λ. The maxima of $L_{0,S}$ for $I = 0.1$ are at $D_F = 16$ and 28, which are not far from 1.5Λ and 2.5Λ, respectively. On the other hand, for $L_{1,S}$ the maxima for $I = 0.1$ are at $D_F = 19$ and 31 and there is a minimum at $D_F = 26$. The locations of these maxima are still near 1.5Λ and 2.5Λ and they are only slightly different than what they are for the $L_{0,S}$ case. If one recalls the above discussion of Fig. 3, maxima of T_c occur when D_F is close to an integer multiple of Λ. Since a higher T_c is correlated with a higher singlet pair amplitude, this suggests again that there exists a conversion between singlet and triplet Cooper pairs. The dependence of $L_{0,S}$ and $L_{1,S}$, at $I = 1.0$, on D_F is harder to characterize. This is because the high value of I reduces the scale of the overall proximity effect in S (i.e., the depletion of the singlet amplitude). At $I = 0.5$, one still finds that the approximate periodicity of $L_{0,S}$ and $L_{1,S}$ is about $\Lambda/2$. The proximity lengths $L_{0,S}$ and $L_{1,S}$ are again anticorrelated at $I = 0.5$: the maxima (minima) locations of $L_{0,S}$ are near the minimum (maximum) locations of $L_{1,S}$.

Recent experiments[33] in systems that consist of two superconducting Nb electrodes coupled via a Ho/Co/Ho trilayer have revealed that the long-range effect of triplet supercurrents was much more prominent at particular thicknesses of the Ho layers. The magnetic coherence length in Ho in the experiment was $\sim$5 nm which would correspond in our notation to $I \sim 0.1$.[56] In the experiment, the Ho thickness was symmetrically varied and the critical current I_c at $T = 4.2$ K was measured. Peaks of I_c corresponding to $D_F = 0.5\Lambda$ and $D_F = 2.5\Lambda$ were found. These experimental findings are consistent with our theory. Here, we have shown (see Fig. 10) that $L_{1,S}$ has maxima near 1.5Λ and 2.5Λ when $I = 0.1$ in the D_F range we have considered. We found another maximum at $D_F \sim 0.5\Lambda$, not included in the range shown. The penetration lengths associated with S are as important as those associated with F when discussing the triplet proximity effect because the system can open up the corresponding channels only when both of them are long ranged. We believe that no obvious peak near 1.5Λ was observed because of the layout of their symmetric system. Therefore, one can conclude that the spiral magnetic structures play an important role in the triplet proximity effects. Both experiment and theory confirm that the existence of the long-range proximity effects depends on the relation between the thickness of the magnetic layers and the wavelength of their magnetic structure.

Having seen in the previous two figures that triplet amplitudes may substantially pervade even rather thick Ho layers at moderate values of τ, it is of interest to investigate the τ

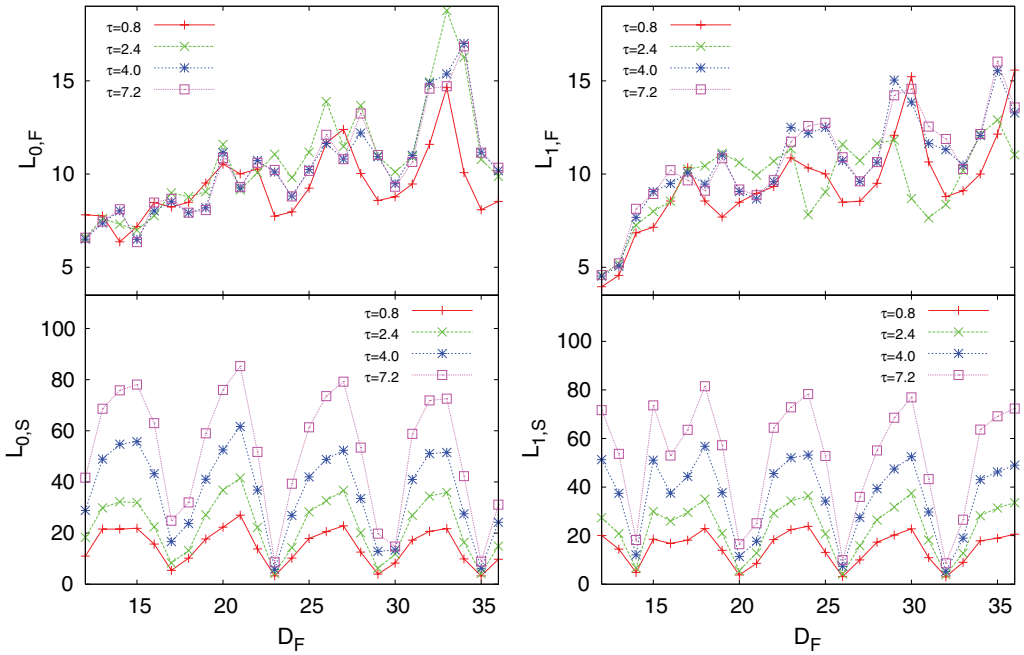

FIG. 11. (Color online) Triplet proximity lengths vs D_F for $I = 0.5$, $D_S = 150$, at different τ values. The left panels show $L_{0,F}$ and $L_{0,S}$, and the right panels show $L_{1,F}$ and $L_{1,S}$. The lines are guides to the eye.

dependence of the proximity lengths in these nanoscale F/S systems for times roughly up to 2π in our dimensionless units. We therefore present in Fig. 11 the triplet proximity lengths as a function of D_F for $I = 0.5$, and at different values of τ. The panel arrangement is as in the previous figure. Thus, in the top panels where we plot $L_{0,F}$ and $L_{1,F}$, we see that both of them depend only weakly on τ, in the range considered. This is in part because of the relatively thin F layers included in the plot. The triplet amplitudes vanish at $\tau = 0$ but can saturate quickly through the F region as soon as τ increases. In contrast, on the much thicker ($D_S = 150$) S side (bottom panels), both $L_{0,S}$ and $L_{1,S}$ increase with τ, as is consistent with expectation and previous work involving F/S systems with misaligned exchange fields.[22] Furthermore, the overall shape of the proximity lengths on the S side does not change with τ and only the magnitude evolves. Quite remarkably, the minima of $L_{0,S}$ and $L_{1,S}$ are very deep, and the value of these lengths at their minima is almost τ independent and nearly the same at all minima in the range plotted. The minima are separated by $\Lambda/2$. If one compares the left and right panels, one can see that the locations of maxima in one approximately coincide with the position of minima in the other: the left and right panels are again complementary to each other as was the case with the plots in Fig. 10.

D. Local magnetization and LDOS

Next, we discuss other important physical quantities that are related to the proximity effects including the local magnetization $\boldsymbol{m}(y)$ and the the local DOS (LDOS). Considering that the ferromagnetism can drastically alter the superconductivity, one might wonder about the opposite case: how the local magnetizations behave near the F/S interface. These so-called reverse proximity effects have been studied[5,17,24,48–53] for a number of multilayer F/S configurations with uniform exchange fields in each magnetic layer. Here, the space-varying exchange fields in F oscillate in the x-z plane and are constant along the y direction (see Fig. 1). We computed the local magnetizations using Eq. (7) for $D_S = 150$, $D_F = \Lambda$, and three different values of I. The results are normalized in the usual[24,51] way so that for a putative bulk F material with a uniform internal field characterized by the parameter I, the quantity plotted would have the value $[(1+I)^{3/2} - (1-I)^{3/2}]/[(1+I)^{3/2} + (1-I)^{3/2}]$. In Fig. 12, each component of $\boldsymbol{m}$ is shown in a separate panel and their behavior plotted throughout the whole spiral magnet region and some distance into S near the interface. Consider first the x component: The corresponding component of the internal field [see Eq. (1)] vanishes at the outer interface ($Y = 0$) and goes smoothly to zero at the F/S interface which in this case is at $Y = D_F = \Lambda$. As a consequence, one can see that the m_x component undergoes a full period of oscillation in the F material. The maximum and minimum values as a function of I are numerically what they should be, given our normalization. However, as Fig. 12 clearly shows, the self-consistently determined m_x does not vanish at the F/S interface and instead penetrates a short distance inside S. This is a manifestation of the reverse proximity effect. For the other transverse component m_z, the situation is more complicated. The field component h_z, out of phase with h_x, does not vanish smoothly at $Y = 0$ nor at $Y = D_F$. Therefore, the corresponding m_z component in F is squeezed, and in addition to the peak at $Y = \Lambda/2$, which has the expected location and value, there are two smaller peaks at intermediate values. At the interface between materials, penetration of this component is appreciably more considerable than for m_x. The longitudinal component m_y, which is induced by the uniform h_y component, behaves qualitatively as transverse components do in uniform ferromagnet F/S structures.[14] Penetration into

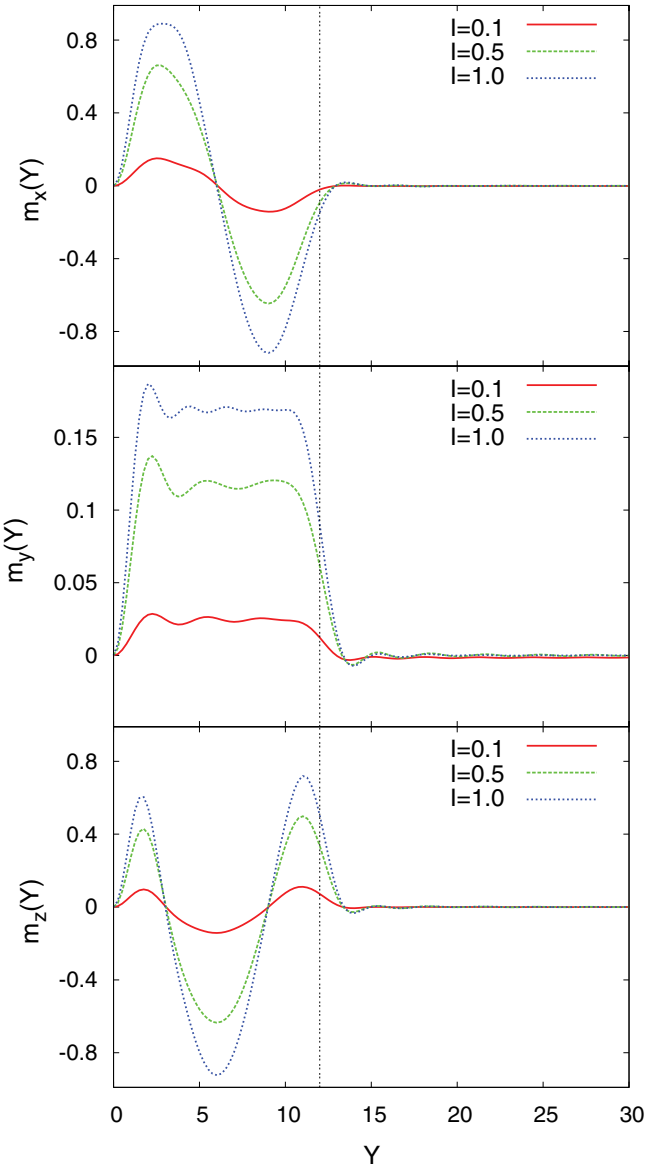

FIG. 12. (Color online) Normalized (see text) local magnetization components plotted as a function of Y for several values of I. From top to bottom, x, y, and z components are shown. We use $D_F = \Lambda$ and $D_S = 150$ in this figure.

the S layer occurs over a relatively short distance, except at the smallest value of I where it is relatively larger although the overall scale is of course smaller. The value of m_y in the F layer is again the expected one, consistent with our normalization.

Finally, we wish to discuss the LDOS. Here, we will present results for the LDOS, as discussed in Sec. II, summed over spins, integrated over either the F or the S layer, and normalized, as usual, to its value in the normal state of bulk S material. The results are given in Fig. 13 where the energy scale of the horizontal axis is in units of the superconducting gap of bulk S material Δ_0. The left panels of Fig. 13 show the LDOS integrated over the F (top) and S regions (bottom) for $D_F = \Lambda$, 1.5Λ, and 2Λ. The superconductor has a thickness $D_S = 1.5\Xi_0$ and F has a relatively weak exchange field $I = 0.1$. For $D_F = \Lambda$, one can clearly see, for the integrated DOS in the S side, peaks near $\varepsilon/\Delta_0 = \pm 1$ as in the ordinary bulk spectrum. There is additional subgap structure including proximity-induced bound states at smaller energies followed by a very deep dip, nearly a minigap. Overall, the DOS structure contains traces of the familiar DOS for a pure bulk superconductor. On the F side, the integrated LDOS at this value of D_F still exhibits BCS-type peaks at $\varepsilon/\Delta_0 = \pm 1$ and subgap dip, but the whole structure is much weaker and the depth of the dip much smaller. It is indicative of the superconducting correlations present in the F region. In contrast, the subgap superconducting features in the integrated LDOS for larger D_F values ($D_F = 1.5\Lambda$ and 2Λ) are much less prominent, although the peaks near $\varepsilon/\Delta_0 = \pm 1$ remain. Nonetheless, there are still shallow and discernible signatures in the gap region, on both the F and S layers. For these two larger values of D_F, the results (as compared on the same side) are remarkably similar. This is surprising at first since we have already seen that $T_c(D_F)$ has in this range of I maxima near $D_F = \Lambda$ and $D_F = 2\Lambda$ and a local minimum at $D_F = 1.5\Lambda$ as shown in Fig. 3. From that, one might naively guess that the integrated LDOS for $D_F = 2\Lambda$ should behave as that at $D_F = \Lambda$, with a different integrated LDOS for $D_F = 1.5\Lambda$. This expectation is incorrect because, as one can see on a closer inspection of Fig. 3, T_c at $D_F = \Lambda$ is higher than that at $D_F = 2\Lambda$ although both are near local maxima. Furthermore, T_c at $D_F = 1.5\Lambda$ is closer to the T_c value at $D_F = 2\Lambda$ than to that at $D_F = \Lambda$. Since T_c is associated with the magnitude of the singlet pair amplitudes, in which the LDOS is indirectly correlated to, one should conclude that the LDOS corresponding to $D_F = 2\Lambda$ should be similar to $D_F = 1.5\Lambda$ rather than $D_F = \Lambda$. Indeed, the results confirm this notion.

On the right panels of Fig. 13, we present the integrated LDOS on both the F and the S sides for different exchange fields $I = 0.1$, 0.5, and 1.0, at $D_F = 12 = \Lambda$. We see that when I is increased from $I = 0.1$, the integrated LDOS on the F side becomes quite flat {at the value $(1/2)[(1+I)^{1/2} + (1-I)^{1/2}]$ as per our normalization} and essentially devoid of a superconducting signature. On the S side, the integrated LDOS at $I = 0.5$ and 1.0 still retains some vestiges of the structure seen in the $I = 0.1$ case. However, the integrated LDOS at $I = 0.5$ on the S side is slightly different than that at $I = 1.0$. The dip at $I = 1.0$ is wider than for $I = 0.5$, in a way more superconductinglike. What happens is that at larger values of I, the mismatch between the Fermi wave vector in S and the Fermi wave vectors in the up and down bands in F increases. This diminishes the penetration of the Cooper pairs into S and hence the overall scale of the proximity effects. We recall that the overall dimensionless scale of the proximity effect in F is roughly $\Xi_F = 1/I$. Consequently, superconductivity is impaired in S over a smaller scale when it is in contact with a stronger ferromagnet. Having said that, one might argue that at $I = 0.1$ the integrated LDOS on the S side should have a smaller dip than the other two curves for stronger I. However, we have to consider here also the overall behavior of the T_c versus I curves at constant D_F. This behavior is once again oscillatory but with a superimposed decay. The overall decay results in T_c being higher at $I = 0.1$ than at either $I = 0.5$ or 1, but the oscillations produce a higher value

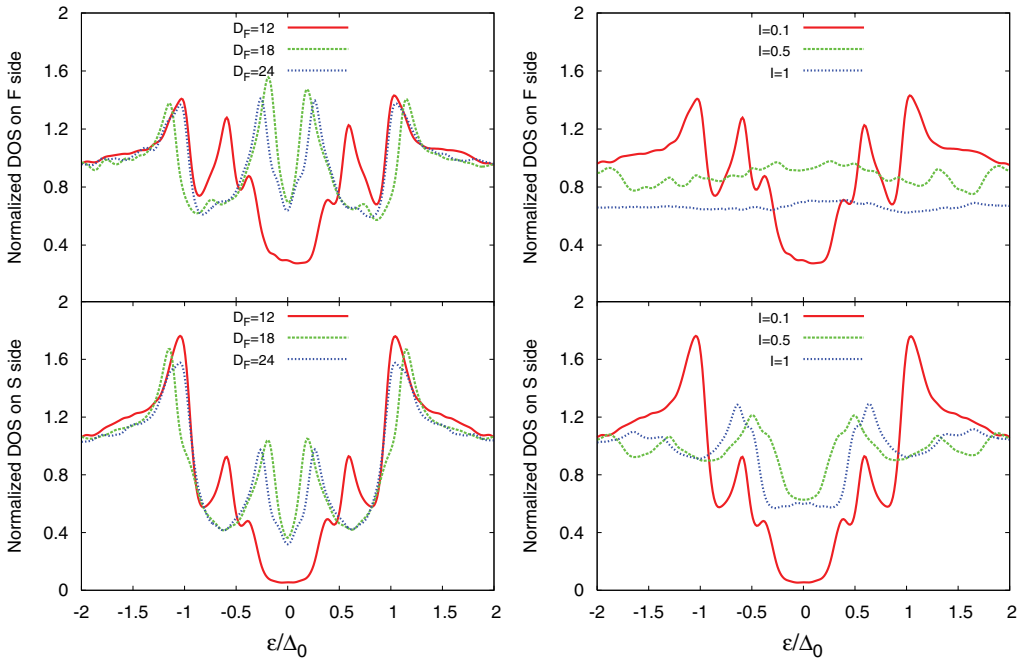

FIG. 13. (Color online) LDOS averaged over the F regions (top panels) and S regions (bottom panels), plotted vs energy. On the left panels, the integrated LDOS is shown for different D_F and $I = 0.1$. On the right panels, the integrated LDOS is shown for different I and $D_F = \Lambda$. In all cases, the superconductor width is set to $D_S = 150$.

of T_c at $I = 1$ than at $I = 0.5$. This explains the progression of the curves. All the above discussion and results indicate that the LDOS can provide, if properly analyzed, another perspective and additional information on the superconducting nature of our bilayers.

IV. CONCLUSIONS

We have studied several aspects of proximity effects in F/S bilayers, where the ferromagnet has a spiral structure characteristic of rare earths such as Ho, by numerically solving the self-consistent BdG equations. We have calculated $T_c(D_F)$, the critical temperature as a function of magnet thickness, for different parameter values. The $T_c(D_F)$ curves exhibit a fairly intricate oscillatory behavior which is found to be related to both the strength I (as they would for a uniform magnet) and the periodicity Λ of the spiral exchange fields inherent in the magnet. As is the case for F/S structures in which F is uniform, we observe reentrant behavior with D_F when I is strong enough. The physical reason behind this D_F reentrance in our bilayers is similar to that in ordinary F/S structures, but the additional periodicity associated with the magnet, which in many cases dominates the oscillations, makes the behavior more complicated. As a function of D_S, we find that $T_c(D_F)$ can also exhibit D_F reentrance even at small I when D_S is of the order of the superconducting coherence length. The additional oscillations produced by the magnetic structure lead also to effects not found in $F_1/F_2/S$ trilayers, namely, pure reentrance with temperature: superconductivity occurs in a finite-temperature range $T_{c1} < T < T_{c2}$. An example of this reentrance at a very small D_F ($D_F \sim 0.5\Lambda$) was previously[38] presented. Here, we report that this reentrance can also occur when $D_F > \Lambda$, where it should be experimentally easier to realize. To elucidate the physics underlying these reentrant phenomena, we have evaluated the singlet pair amplitudes and thermodynamic functions. The competition between condensation energy and entropy is responsible for the T reentrance: the superconducting state may be, under certain circumstances, the high-entropy state, leading to recovery of the normal state as T is lowered. The calculated thermodynamic quantities are fully consistent with the $T_c(D_F)$ phase diagrams and the singlet pair amplitudes.

When the magnet has a spiral structure, both the $m = 0$ and ± 1 odd triplet components can be induced simultaneously. This is not the case in uniform-magnet bilayers: at least two uniform misaligned F layers are needed to generate the $m = \pm 1$ component. We studied the odd triplet pair amplitudes in our bilayers, and found them to be long ranged in both the S and F layers. We have analyzed the time-delay dependence of the odd triplet amplitudes. The results are consistent with our previous work on both $F_1/S/F_2$ and $F_1/F_2/S$ trilayers, but the additional Λ periodicity leads to important differences. We characterized the triplet long-range behavior by introducing the appropriately defined lengths. We found that the relevant proximity length oscillates with D_F and these oscillations depend on the strength and periodicity of the exchange field. Our methods are likely appropriate for many experimental conditions, as evidenced by the consistency of our results with recent tunneling experiments.[33]

We have also considered the reverse proximity effects: the influence of the superconductivity on the magnetism. We found all three components of the local magnetization penetrate in slightly different ways into the S layer. At larger I, this is a short-ranged phenomenon, but it is otherwise for weak

magnetism. Both m_x and m_z oscillate in the F regions to reflect the spiral exchange field. Finally, the calculated LDOS reveals important information and discernible signatures linked to the proximity effects in these bilayers and are correlated to the superconducting transition temperatures.

ACKNOWLEDGMENTS

We thank C. Grasse for technical support. K.H. is supported in part by ONR and grants of computing resources from DoD (HPCMP). O.T.V. and C.-T. Wu are supported in part by IARPA under Grant No. N66001-12-1-2023.

*wu@physics.umn.edu

†Also at Minnesota Supercomputer Institute, University of Minnesota, Minneapolis, Minnesota 55455; otvalls@umn.edu

‡klaus.halterman@navy.mil

[1] I. Žutić, J. Fabian, and S. Das Sarma, Rev. Mod. Phys. **76**, 323 (2004).

[2] F. S. Bergeret, A. F. Volkov, and K. B. Efetov, Rev. Mod. Phys. **77**, 1321 (2005).

[3] A. I. Buzdin, Rev. Mod. Phys. **77**, 935 (2005).

[4] E. A. Demler, G. B. Arnold, and M. R. Beasley, Phys. Rev. B **55**, 15174 (1997).

[5] K. Halterman and O. T. Valls, Phys. Rev. B **65**, 014509 (2001).

[6] I. A. Garifullin, D. A. Tikhonov, N. N. Garifyanov, L. Lazar, Y. V. Goryunov, S. Y. Khlebnikov, L. R. Tagirov, K. Westerholt, and H. Zabel, Phys. Rev. B **66**, 020505(R) (2002).

[7] V. Zdravkov, A. Sidorenko, G. Obermeier, S. Gsell, M. Schreck, C. Muller, S. Horn, R. Tidecks, and L. R. Tagirov, Phys. Rev. Lett. **97**, 057004 (2006).

[8] V. I. Zdravkov, J. Kehrle, G. Obermeier, S. Gsell, M. Schreck, C. Müller, H.-A. Krug von Nidda, J. Lindner, J. Moosburger-Will, E. Nold, R. Morari, V. V. Ryazanov, A. S. Sidorenko, S. Horn, R. Tidecks, and L. R. Tagirov, Phys. Rev. B **82**, 054517 (2010).

[9] Z. Radović, M. Ledvij, L. Dobrosavljevic-Grujic, A. I. Buzdin, and J. R. Clem, Phys. Rev. B **44**, 759 (1991).

[10] M. G. Khusainov and Y. N. Proshin, Phys. Rev. B **56**, R14283 (1997).

[11] Y. V. Fominov, N. M. Chtchelkatchev, and A. A. Golubov, Phys. Rev. B **66**, 014507 (2002)

[12] I. Baladié and A. Buzdin, Phys. Rev. B **67**, 014523 (2003).

[13] K. Halterman and O. T. Valls, Phys. Rev. B **70**, 104516 (2004).

[14] K. Halterman and O. T. Valls, Phys. Rev. B **72**, 060514(R) (2005).

[15] M. Eschrig and T. Löfwander, Nat. Phys. **4**, 138 (2008).

[16] M. Eschrig, J. Kopu, J. C. Cuevas, and G. Schön, Phys. Rev. Lett. **90**, 137003 (2003); M. Eschrig, T. Löfwander, T. Champel, J. C. Cuevas, J. Kopu, and G. Schön, J. Low Temp. Phys. **147**, 457 (2007).

[17] K. Halterman and O. T. Valls, Phys. Rev. B **80**, 104502 (2009).

[18] F. S. Bergeret, A. F. Volkov, and K. B. Efetov, Phys. Rev. Lett. **86**, 3140 (2001).

[19] F. S. Bergeret, A. F. Volkov, and K. B. Efetov, Phys. Rev. B **68**, 064513 (2003).

[20] T. Löfwander, T. Champel, J. Durst, and M. Eschrig, Phys. Rev. Lett. **95**, 187003 (2005).

[21] K. Halterman, P. H. Barsic, and O. T. Valls, Phys. Rev. Lett. **99**, 127002 (2007).

[22] K. Halterman, O. T. Valls, and P. H. Barsic, Phys. Rev. B **77**, 174511 (2008).

[23] V. L. Berezinskii, Pis'ma v ZhETF **20**, 628 (1974) [JETP Lett. **20**, 287 (1974)].

[24] C.-T. Wu, O. T. Valls, and K. Halterman, Phys. Rev. B **86**, 014523 (2012).

[25] T. S. Khaire, M. A. Khasawneh, W. P. Pratt, Jr., and N. O. Birge, Phys. Rev. Lett. **104**, 137002 (2010).

[26] J. Y. Gu, J. Kusnadi, and C.-Y. You, Phys. Rev. B **81**, 214435 (2010).

[27] D. Sprungmann, K. Westerholt, H. Zabel, M. Weides, and H. Kohlstedt, Phys. Rev. B **82**, 060505 (2010).

[28] A. F. Volkov, A. Anishchanka, and K. B. Efetov, Phys. Rev. B **73**, 104412 (2006).

[29] I. Sosnin, H. Cho, V. T. Petrashov, and A. F. Volkov, Phys. Rev. Lett. **96**, 157002 (2006).

[30] J. W. Cable, E. O. Wollan, W. C. Koehler, and M. K. Wilkinson, Phys. Rev. **140**, A1896 (1965).

[31] E. A. Karhu, S. Kahwaji, M. D. Robertson, H. Fritzsche, B. J. Kirby, C. F. Majkrzak, and T. L. Monchesky, Phys. Rev. B **84**, 060404 (2011).

[32] H. Shi, Z.-B. Huang, J. S. Tse, and H.-Q. Lin, J. Appl. Phys. **110**, 043917 (2011).

[33] J. W. A. Robinson, J. D. S. Witt, and M. G. Blamire, Science **329**, 59 (2010).

[34] M. Alidoust, J. Linder, G. Rashedi, T. Yokoyama, and A. Sudbø, Phys. Rev. B **81**, 014512 (2010).

[35] M. Alidoust and J. Linder, Phys. Rev. B **82**, 224504 (2010).

[36] G. B. Halász, M. G. Blamire, and J. W. A. Robinson, Phys. Rev. B **84**, 024517 (2011).

[37] G. B. Halász, J. W. A. Robinson, J. F. Annett, and M. G. Blamire, Phys. Rev. B **79**, 224505 (2009).

[38] C.-T. Wu, O. T. Valls, and K. Halterman, Phys. Rev. Lett. **108**, 117005 (2012).

[39] W. A. Fertig, D. C. Johnston, L. E. DeLong, R. W. McCallum, M. B. Maple, and B. T. Matthias, Phys. Rev. Lett. **38**, 987 (1977).

[40] D. E. Moncton, D. B. McWhan, J. Eckert, G. Shirane, and W. Thomlinson, Phys. Rev. Lett. **39**, 1164 (1977).

[41] H. R. Ott, W. A. Fertig, D. C. Johnston, M. B. Maple, and B. T. Matthias, J. Low Temp. Phys. **33**, 159 (1978).

[42] G. W. Crabtree, F. Behroozi, S. A. Campbell, and D. G. Hinks, Phys. Rev. Lett. **49**, 1342 (1982).

[43] J. W. Lynn, J. A. Gotaas, R. N. Shelton, H. E. Horng, and C. J. Glinka, Phys. Rev. B **31**, 5756 (1985).

[44] P. G. de Gennes, *Superconductivity of Metals and Alloys* (Addison-Wesley, Reading, Massachusetts, 1989).

[45] The phase convention used here is that of, e.g., Ref. 38. Other conventions may lead to slightly different signs in the equations.

[46] P. H. Barsic, O. T. Valls, and K. Halterman, Phys. Rev. B **75**, 104502 (2007).

[47] I. Kosztin, S. Kos, M. Stone, and A. J. Leggett, Phys. Rev. B **58**, 9365 (1998).

[48] A. Frydman and R. C. Dynes, Phys. Rev. B **59**, 8432 (1999).
[49] V. N. Krivoruchko and E. A. Koshina, Phys. Rev. B **66**, 014521 (2002).
[50] F. S. Bergeret, A. F. Volkov, and K. B. Efetov, Phys. Rev. B **69**, 174504 (2004).
[51] K. Halterman and O. T. Valls, Phys. Rev. B **69**, 014517 (2004).
[52] F. S. Bergeret, A. Levy Yeyati, and A. Martín-Rodero, Phys. Rev. B **72**, 064524 (2005).
[53] M. Yu. Kharitonov, A. F. Volkov, and K. B. Efetov, Phys. Rev. B **73**, 054511 (2006).
[54] J. Linder, T. Yokoyama, and A. Sudbø, Phys. Rev. B **79**, 054523 (2009).
[55] J. Zhu, I. N. Krivorotov, K. Halterman, and O. T. Valls, Phys. Rev. Lett. **105**, 207002 (2010).
[56] F. Chiodi, J. D. S. Witt, R. G. J. Smits, L. Qu, G. B. Halász, C.-T. Wu, O. T. Valls, K. Halterman, J. W. A. Robinson, and M. G. Blamire, arXiv:1211.1169 [Europhysics Letters (to be published)].
[57] P. W. Anderson and H. Suhl, Phys. Rev. **116**, 898 (1959).